

Electronic Supplementary Information for  
**Amorphous-crystalline PdRu bimetallic for efficient hydrogen evolution  
electrocatalysis**

Hongjing Wang, Beibei Wang, Hongjie Yu, Peng Wang, Kai Deng, You Xu, Xin Wang,

Ziqiang Wang\* and Liang Wang\*

State Key Laboratory Breeding Base of Green-Chemical Synthesis Technology, College of  
Chemical Engineering, Zhejiang University of Technology, Hangzhou 310014, P. R. China

**\* Corresponding authors**

\*E-mails:

zqwang@zjut.edu.cn;

wangliang@zjut.edu.

## Experimental section

**Materials and chemicals:** Palladium (II) acetylacetonate ( $\text{Pd}(\text{acac})_2$ ), ruthenium trichloride ( $\text{RuCl}_3$ ) and Nafion solution (5 wt%) were purchased from Sigma-Aldrich. Tungsten hexacarbonyl ( $\text{W}(\text{CO})_6$ ), N,N-dimethylformamide (DMF), acetic acid ( $\text{CH}_3\text{COOH}$ ) and ethanol ( $\text{C}_2\text{H}_5\text{OH}$ ) were bought from Aladdin. Commercial Pt/C (20 wt %) catalyst was purchased from Alfa Aesar.

**Synthesis of samples:** For the preparation of PdRu bimetallic, 10 mg of  $\text{Pd}(\text{acac})_2$ , 5 mg of  $\text{RuCl}_3$  and 10 mg of  $\text{W}(\text{CO})_6$  were dissolved in 8 mL of DMF under ultrasonic conditions, followed by adding 2 mL of acetic acid, which was heated at 75 °C for 2 h. The as-obtained product was collected by centrifugation and washed with ethanol for five cycles, which was dried at 50 °C for further use. For comparison, the Pd metallic was synthesized from the absence of Ru precursors under the similar condition.

**Characterization:** The morphology of samples was characterized by scanning electron microscope (SEM, Zeiss Gemini 500). Transmission electron microscopy (TEM) equipped with energy-dispersive X-ray spectroscopy (EDX), high-angle annular dark-field scanning TEM (HAADF-STEM), high-resolution TEM (HRTEM), and elemental mapping images were conducted by a JEOL JEM-2100F microscope. Atomic force microscopy (AFM) was recorded by Bruker Dimension ICON. X-ray diffraction (XRD) pattern of samples was obtained by a DX-2700 diffractometer. The element composition and electronic state of samples were determined by X-ray photoelectron spectroscopy (XPS, ULVAC PHI Quantera) measurements.

**Electrochemical measurements:** The electrochemical measurement was carried on the CHI 760E electrochemical workstation in an H-type battery separated by a Nafion 211 membrane using three-electrode system. Graphite rod and Ag/AgCl electrode (3 M KCl) were served as counter electrode and reference electrode, respectively. To fabricate working electrode, the catalyst ink was prepared

by dispersing 2 mg of catalyst into 800  $\mu\text{L}$  of  $\text{H}_2\text{O}$ , 100  $\mu\text{L}$  of isopropanol and 100  $\mu\text{L}$  of Nafion (0.5 wt%) under sonication, and then 5  $\mu\text{L}$  or 200  $\mu\text{L}$  of catalyst ink was dropped on the glassy carbon electrode ( $0.071\text{ cm}^2$ ) or carbon paper ( $1\text{ cm}^2$ ), respectively, followed by drying in an oven at  $50\text{ }^\circ\text{C}$ . The electrolytes ( $0.5\text{ M H}_2\text{SO}_4$ ) purged with nitrogen before electrochemical measurements. The linear sweep voltammetry (LSV) curves with  $iR$  compensation were performed at a sweep rate of  $5\text{ mV s}^{-1}$ . The chronopotentiometric test was performed for 12 h at a current density of  $-10\text{ mA cm}^{-2}$ . Electrochemical impedance spectroscopy (EIS) measurements were conducted in the frequency range from 100 kHz to 1 Hz at  $-30\text{ mV}$ . The diameter of the semicircle in the high frequency region represents the charge transfer resistance ( $R_{ct}$ ). The intersection value of the low frequency region with  $Z''=0$  represents the solution resistance ( $R_s$ ), which is attributed to the ohmic resistance of the electrolyte and electrocatalyst. The Faraday efficiency was calculated by using the ratio of measured hydrogen amounts by the drainage method to theoretical hydrogen amounts. All potentials were transformed to reversible hydrogen electrode (RHE) and current density was normalized to the geometric area of the glassy carbon electrode or carbon paper.

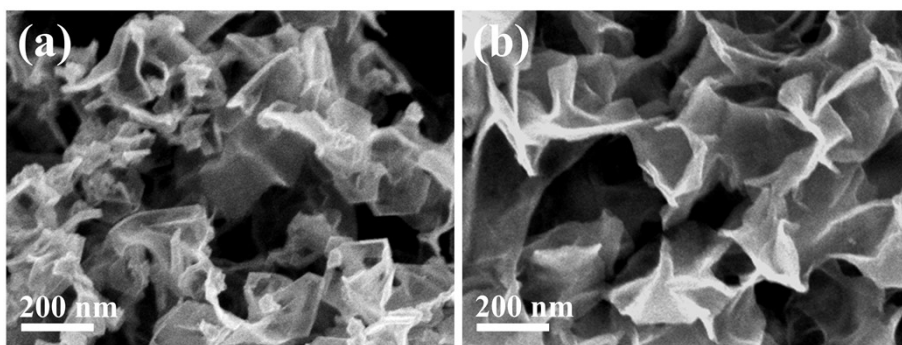


**Fig. S1** SEM images of (a) Pd metallene and (b) PdRu bimetallene.

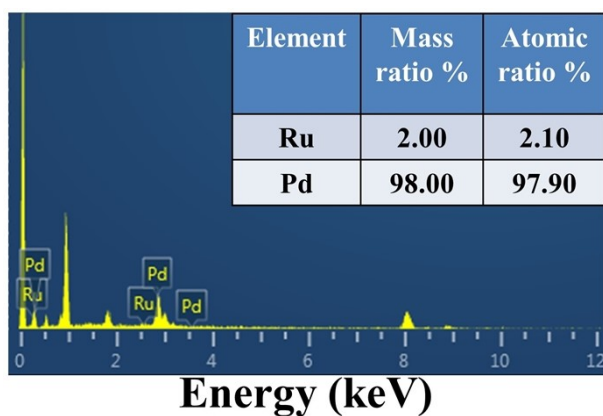


**Fig. S2** EDX spectrum of the PdRu bimetallene.

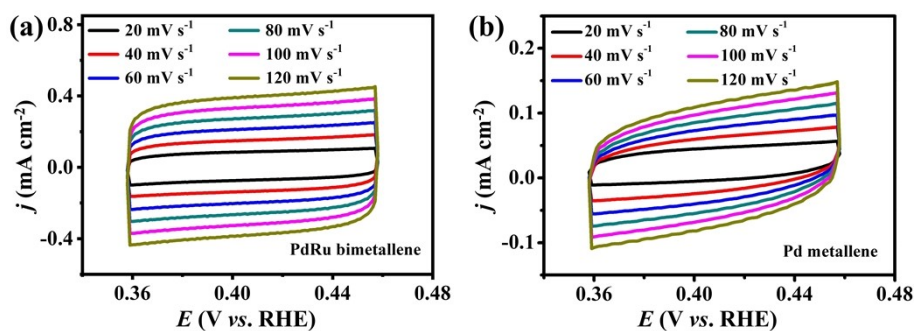


**Fig. S3** CV curves with different scan rates for different catalysts.

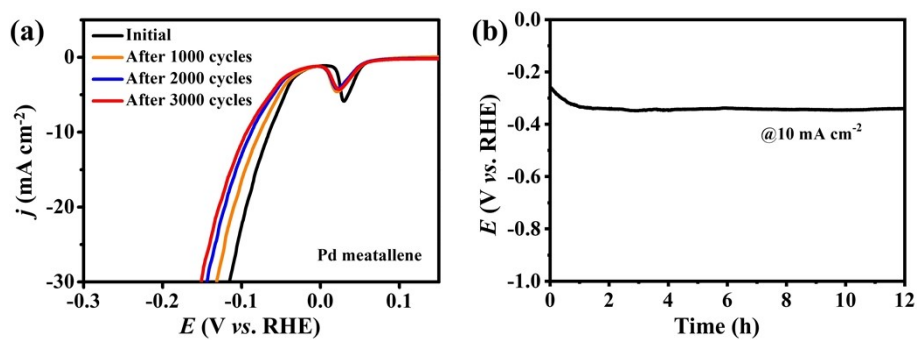


**Fig. S4** (a) LSV curves of the Pd metallene before and after 3000 cycles. (b) Chronopotentiometric curve without  $iR$  compensation of Pd metallene at  $-10 \text{ mA cm}^{-2}$  for 12 h.

**Table S1.** Comparison of HER activity for the PdRu bimetallic and some other reported electrocatalysts.

Catalyst	Overpotential at -10 mA cm <sup>-2</sup> (mV)	Tafel slop (mV dec <sup>-1</sup> )	Electrolyte	Ref.
<b>PdRu bimetallic</b>	<b>32</b>	<b>32.3</b>	<b>0.5 M H<sub>2</sub>SO<sub>4</sub></b>	<b>This work</b>
<i>fcc</i> -Pd <sub>47</sub> @Ir <sub>53</sub>	48.5	75	0.5 M H <sub>2</sub> SO <sub>4</sub>	1
Ru@C	63	47	0.5 M H <sub>2</sub> SO <sub>4</sub>	2
RuRh <sub>2</sub> bimetallic	34	17	0.5 M H <sub>2</sub> SO <sub>4</sub>	3
H-PtNiCu-AAT	32	33	0.1 M HClO <sub>4</sub>	4
CS-PdPt	26	33	0.5 M H <sub>2</sub> SO <sub>4</sub>	5
Au <sub>75</sub> Rh <sub>25</sub>	64.1	33.8	0.5 M H <sub>2</sub> SO <sub>4</sub>	6
Rh NP@BNS	66	56	0.5 M H <sub>2</sub> SO <sub>4</sub>	7
P-Pd <sub>4</sub> S NWs	47	32.7	0.5 M H <sub>2</sub> SO <sub>4</sub>	8
np-Ru	74	51	0.5 M H <sub>2</sub> SO <sub>4</sub>	9
RhSe <sub>2</sub>	49.9	39	0.5 M H <sub>2</sub> SO <sub>4</sub>	10

## References

- 1 Y. Ge, X. Wang, B. Chen, Z. Huang, Z. Shi, B. Huang, J. Liu, G. Wang, Y. Chen, L. Li, S. Lu, Q. Luo, Q. Yun and H. Zhang, *Adv. Mater.*, 2022, **34**, 2107399.
- 2 H. Zhang, W. Zhou, X. F. Lu, T. Chen and X. W. Lou, *Adv. Energy Mater.*, 2020, **10**, 2000882.
- 3 X. Mu, J. Gu, F. Feng, Z. Xiao, C. Chen, S. Liu and S. Mu, *Adv. Sci.*, 2021, **8**, 2002341.
- 4 D. Wu, W. Zhang, A. Lin and D. Cheng, *ACS Appl. Mater. Interfaces*, 2020, **12**, 9600-9608.
- 5 B. T. Jebaslinhepzybai, N. Prabu and M. Sasidharan, *Int. J. Hydrogen Energy*, 2020, **45**, 11127-11137.
- 6 T. Bian, B. Xiao, B. Sun, L. Huang, S. Su, Y. Jiang, J. Xiao, A. Yuan, H. Zhang and D. Yang, *Appl. Catal., B*, 2020, **263**, 118255.
- 7 K. Chen, Z. Wang, L. Wang, X. Wu, B. Hu, Z. Liu and M. Wu, *Nano-Micro Lett.*, 2021, **13**, 138.
- 8 C. Li, Y. Xu, H. Yu, K. Deng, S. Liu, Z. Wang, X. Li, L. Wang and H. Wang, *Nanotechnology*, 2020, **31**, 045401.
- 9 A. S. B. Mohd Najib, M. Iqbal, M. B. Zakaria, S. Shoji, Y. Cho, X. Peng, S. Ueda, A. Hashimoto, T. Fujita, M. Miyauchi, Y. Yamauchi and H. Abe, *J. Mater. Chem. A*, 2020, **8**, 19788-19792.
- 10 W. Zhong, B. Xiao, Z. Lin, Z. Wang, L. Huang, S. Shen, Q. Zhang and L. Gu, *Adv. Mater.*, 2021, **33**, 2007894.